Development and Evaluation of a Thermosensitive Intravesical in-Situ Hydrogel Incorporating Nitrofurantoin Nanocrystals for Sustained Localized Therapy of Recurrent Urinary Tract Infections

Katari Anchal Mannath[1], V. Phanideepthi[2]*, K. Veena[3], K. Kishore Rathna Prasad[4]

[1]Student, Department of Pharmaceutics, JNTUA–Oil Technological & Pharmaceutical Research Institute (JNTUA–OTPRI), Anantapur, Andhra Pradesh, India

[2]Assistant Professor, Department of Pharmaceutics, JNTUA–Oil Technological & Pharmaceutical Research Institute (JNTUA–OTPRI), Anantapur, Andhra Pradesh, India

[3]Assistant Professor, Department of Pharmacy Practice, JNTUA–Oil Technological & Pharmaceutical Research Institute (JNTUA–OTPRI), Anantapur, Andhra Pradesh, India

[4]Assistant professor, Department of Pharmaceutics, MIPER, Kurnool.

Corresponding Author:

V. Phanideepthi

Assistant Professor, Department of Pharmaceutics,

JNTUA–Oil Technological & Pharmaceutical Research Institute (JNTUA–OTPRI),

Anantapur, Andhra Pradesh, India.

Email ID: vphanideepthi@gmail.com

Phone: +91 84990 27258

ABSTRACT

Background: Recurrent urinary tract infections (rUTIs) represent a significant global health challenge, affecting approximately 50-60% of women worldwide with high recurrence rates. Conventional oral antibiotic therapy is limited by systemic side effects, poor patient compliance, and the escalating crisis of antimicrobial resistance, necessitating the development of advanced localized delivery systems. **Objective:** This study aimed to develop, optimize, and comprehensively evaluate a novel thermosensitive mucoadhesive in-situ hydrogel incorporating nitrofurantoin nanocrystals (NFT-NS) for prolonged intravesical therapy of rUTIs, addressing the limitations of current treatment modalities. **Methods:** A Quality by Design approach utilizing Box-Behnken Design was employed to optimize Poloxamer 407-chitosan based hydrogels loaded with NFT-NS. The optimized formulation (OPT-1) underwent extensive characterization including physicochemical properties, rheological behavior, mucoadhesive strength, in vitro drug release kinetics, ex vivo permeation studies, antimicrobial efficacy against uropathogenic E. coli, intracellular killing assessment in human bladder epithelial cells, and comprehensive stability studies. **Results:** The optimized formulation OPT-1 (18.7% P407, 0.43% CS, 2.1% NFT) demonstrated ideal thermosensitive properties with gelation at 34.1 ± 0.5°C occurring within 42 ± 4 seconds. NFT nanocrystals exhibited a mean particle size of 168 ± 9 nm with narrow distribution (PDI 0.12 ± 0.03) and significantly enhanced saturation solubility (381 ± 12 µg/mL, 18-fold increase). The hydrogel showed pronounced pseudoplastic behavior with 5.1-fold enhanced mucoadhesive strength (82.6 ± 5.1 mN/cm²) compared to P407-only gels. Sustained zero-order drug release (93.8 ± 2.1% over 12 hours, R^2=0.997) following anomalous transport mechanism was observed. OPT-1 demonstrated superior antimicrobial activity with larger zone of inhibition (29.8 ± 1.1 mm), lower MIC (4 µg/mL), and remarkable 3.2-log reduction in intracellular bacterial load compared to 0.9-log reduction with conventional suspension. Ex vivo studies revealed 4.8-fold higher mucosal deposition with 89% reduction in systemic flux. The formulation maintained excellent stability over 6 months under refrigerated conditions. **Conclusion:** The successfully developed intravesical hydrogel platform represents a transformative approach for rUTI management through sustained localized delivery, enhanced mucoadhesion, superior efficacy against both planktonic and intracellular bacteria, and minimized systemic exposure. This advanced drug delivery system addresses critical limitations of current therapies and offers significant potential for improving patient outcomes while combating antimicrobial resistance.

Keywords: Intravesical drug delivery, In-situ hydrogel, Thermosensitive, Nitrofurantoin nanocrystals, Quality by Design,

How to cite this article: Mannath KA, Phanideepthi V, Veena K, Prasad KKR. Development and Evaluation of a Thermosensitive Intravesical in-Situ Hydrogel Incorporating Nitrofurantoin Nanocrystals for Sustained Localized Therapy of Recurrent Urinary Tract Infections. Int J Drug Deliv Technol. 2026;16(62s): 1241-1256. DOI: 10.25258/ijddt.16.62s.131

Source of support: Nil.

**Author for Correspondence:* vphanideepthi@gmail.com

Conflict of interest: Nil.

INTRODUCTION

Urinary tract infections (UTIs) represent one of the most prevalent bacterial infections worldwide, constituting a substantial burden on healthcare systems and significantly impacting patients' quality of life. Current epidemiological data indicates that approximately 50-60% of adult women experience at least one UTI episode during their lifetime, with a considerable subset—25-40%—progressing to recurrent UTIs (rUTIs), defined as at least three confirmed episodes within twelve months or two episodes within six months [1]. The management and prevention of rUTIs present formidable clinical challenges that extend beyond acute infection treatment to encompass long-term prophylactic strategies and quality of life considerations.

The conventional mainstay of rUTI management, oral antibiotic therapy, faces increasing limitations in the contemporary healthcare landscape. Repeated and prolonged antibiotic administration, often necessary for effective prophylaxis, contributes significantly to the development of antimicrobial resistance (AMR), recognized by the World Health Organization as one of the top ten global public health threats [2]. Furthermore, oral therapy is associated with systemic side effects including gastrointestinal disturbances, hepatotoxicity, pulmonary complications, and disruption of natural microbiota, which collectively compromise patient compliance and treatment efficacy [3]. The pharmacological limitations of many first-line UTI antibiotics, particularly issues of poor solubility and inadequate bladder tissue penetration, further constrain their therapeutic potential.

Nitrofurantoin, a broad-spectrum nitrofuran derivative, has maintained its position as a first-line agent for treating uncomplicated lower UTIs due to its continued efficacy against common uropathogens, favorable safety profile compared to alternatives, and relatively low resistance rates [4]. However, its clinical utility is substantially limited by poor aqueous solubility characteristics, classifying it as Biopharmaceutical Classification System (BCS) Class II, which results in dissolution rate-limited absorption and variable bioavailability [5]. Additionally, long-term administration for prophylaxis is associated with potential adverse effects including peripheral neuropathy, hepatic toxicity, and pulmonary reactions, particularly in elderly populations and patients with compromised renal function [6].

Localized intravesical drug delivery has emerged as a promising strategic alternative to overcome the limitations of systemic therapy. This approach involves the direct instillation of therapeutic agents into the bladder lumen via catheterization, enabling the achievement of high local drug concentrations at the primary infection site while virtually eliminating systemic exposure and associated side effects [7]. The targeted nature of this delivery route also reduces the selective pressure for antimicrobial resistance development in commensal flora and other body sites. However, traditional intravesical solutions face the significant challenge of rapid clearance during the first voiding cycle, typically within 1-2 hours post-instillation, necessitating frequent catheterizations that are invasive, uncomfortable, and impractical for long-term management [8].

In-situ forming hydrogels represent an advanced technological solution to address the residence time limitations of conventional intravesical formulations. These sophisticated delivery systems are administered as liquids that undergo rapid sol-to-gel transition upon exposure to physiological conditions within the bladder environment, primarily temperature (37°C) and pH, forming a sustained-release depot that adheres to the urothelium [9]. This transformation from solution to gel state significantly prolongs residence time, protects the incorporated drug from premature clearance, and enables controlled release over extended periods, potentially aligning with normal voiding intervals.

Poloxamer 407 (P407), a synthetic triblock copolymer composed of poly(ethylene oxide)-poly(propylene oxide)-poly(ethylene oxide), has been extensively investigated for thermosensitive in-situ gelling applications due to its reversible thermal gelation properties, excellent biocompatibility, and established regulatory acceptance [10]. However, hydrogels based exclusively on P407 often demonstrate limitations including relatively rapid erosion rates in the dynamic bladder environment and insufficient mucoadhesive properties to withstand urinary flow, resulting in suboptimal residence times.

Chitosan, a natural biodegradable polysaccharide derived from chitin, presents as an ideal complementary polymer to augment P407-based systems. Its cationic nature facilitates strong mucoadhesive interactions with the anionic sialic acid residues abundantly present on bladder mucosal surfaces, significantly enhancing residence time [11]. Additionally, chitosan possesses inherent antimicrobial properties against a broad spectrum of pathogens and permeation-enhancing capabilities that may improve drug penetration into bladder tissues and intracellular compartments where bacterial reservoirs often persist [12].

The integration of drug nanocrystal technology represents a cutting-edge formulation strategy to address the solubility limitations of nitrofurantoin. Nanocrystal formulations enhance dissolution rate and apparent solubility through substantial increases in surface area and alteration of surface properties, potentially overcoming the dissolution-limited bioavailability that constrains conventional

nitrofurantoin formulations [13]. This approach is particularly advantageous for intravesical delivery where drug dissolution in urine is critical for therapeutic efficacy.

While previous research has explored individual components of this proposed system, a comprehensive integrated approach combining nanocrystal technology with systematically optimized thermosensitive mucoadhesive hydrogels specifically designed for intravesical nitrofurantoin delivery remains unreported in the scientific literature. This study employs a rigorous Quality by Design (QbD) framework to develop, optimize, and thoroughly characterize a novel intravesical drug delivery platform that synergistically combines nitrofurantoin nanocrystals with optimized P407-chitosan hydrogels. The systematic approach ensures a robust understanding of critical material attributes and process parameters affecting product performance, ultimately yielding an optimized formulation with well-defined design space.

The specific objectives of this comprehensive investigation include: (1) Application of Box-Behnken Design for systematic formulation optimization and design space establishment; (2) Comprehensive physicochemical, rheological, and functional characterization of the optimized system; (3) Detailed evaluation of drug release kinetics and transport mechanisms; (4) Quantitative assessment of mucoadhesive properties and tissue interactions; (5) Investigation of antimicrobial efficacy against planktonic and biofilm-associated bacteria; (6) Evaluation of intracellular bacterial killing potential in relevant cell culture models; and (7) Comprehensive stability profiling under various storage conditions.

MATERIALS AND METHODS:

2.1. Materials

Nitrofurantoin (NFT, pharmaceutical grade, ≥99% purity) was generously provided as a gift sample by Aurobindo Pharma Ltd. (Hyderabad, India). Poloxamer 407 (Kolliphor® P407, Pharmaceutically approved grade) was procured from BASF India Ltd. (Mumbai, India). Chitosan (low molecular weight, 85% deacetylated) and all chemical reagents including glacial acetic acid, solvents, and buffer components were purchased from Sigma-Aldrich (Bangalore, India). All chemicals and solvents utilized were of analytical reagent grade unless otherwise specified. Cell culture reagents, media, and supplements for biological studies were obtained from Himedia Laboratories (Mumbai, India). Simulated Urinary Fluid (SUF) was prepared fresh according to established formulations reported in literature [14]. Uropathogenic Escherichia coli (ATCC® 25922™) and human bladder epithelial cells (5637 cell line) were acquired from authenticated culture collections and maintained according to standard protocols.

2.2. Preparation of Nitrofurantoin Nanocrystals (NFT-NS)

NFT nanocrystals were fabricated using an optimized antisolvent precipitation technique followed by controlled ultrasonication, as previously reported with modifications [15]. Briefly, a concentrated NFT solution was prepared by dissolving the drug in dimethyl sulfoxide (DMSO) at a concentration of 20 mg/mL under magnetic stirring at 500 rpm. This organic phase was rapidly injected (1 mL/min) using a syringe pump into an aqueous antisolvent phase consisting of Poloxamer 188 (0.5% w/v) as stabilizer, maintained at 4°C under high-speed magnetic stirring (1000 rpm) to ensure rapid mixing and nucleation. The resulting pre-suspension was immediately subjected to probe ultrasonication (Sonics Vibra-Cell VCX 750, 40 kHz frequency, 150 W power) for 15 minutes with a 5-second pulse/5-second pause cycle while maintained in an ice bath to prevent temperature rise and Ostwald ripening. The nanocrystals were separated by centrifugation at 15,000 rpm for 20 minutes, washed twice with distilled water to remove excess stabilizer and solvent residues, and subsequently redispersed in an appropriate volume of distilled water for further characterization and incorporation into hydrogel formulations.

2.3. Experimental Design and Optimization

A three-factor, three-level Box-Behnken Design (BBD) was employed for systematic formulation optimization using Design-Expert® software (Version 13, Stat-Ease Inc., Minneapolis, MN, USA). This response surface methodology design was selected for its efficiency in estimating quadratic response surfaces with a reduced number of experimental runs compared to full factorial designs. The independent variables selected based on preliminary screening studies included: Poloxamer 407 concentration (X_1: 16, 18, 20% w/v), Chitosan concentration (X_2: 0.2, 0.4, 0.6% w/v), and NFT loading (X_3: 1, 2, 3% w/v). The dependent responses identified as Critical Quality Attributes (CQAs) included: Gelation temperature (Y_1, target range: 33-35°C), Gelation time (Y_2, target: <60 seconds), Mucoadhesive strength (Y_3, target: maximize), and Cumulative drug release at 12 hours (Y_4, target: >90%). Seventeen experimental runs, including five center points for estimation of pure error, were generated and executed in randomized order to minimize bias.

2.4. Preparation of In-Situ Forming Hydrogels

Thermosensitive in-situ hydrogels were prepared using the established cold method with appropriate modifications [16]. Calculated amounts of P407 were slowly dispersed in cold distilled water (4°C) under continuous magnetic stirring at 500 rpm until complete dissolution and formation of a clear solution, typically requiring 4-6 hours. Chitosan

was dissolved separately in 1% v/v aqueous acetic acid solution with stirring overnight to ensure complete dissolution. The two polymer solutions were then mixed homogeneously under gentle stirring in an ice bath to prevent premature gelation. The previously prepared NFT nanocrystal suspension was subsequently incorporated and uniformly dispersed using a magnetic stirrer at low speed. The final volume was adjusted with cold distilled water, and the formulations were stored at 4°C for 24 hours to ensure complete polymer hydration and removal of entrapped air bubbles. All hydrogel formulations were protected from light during preparation and storage.

2.5. Characterization of NFT Nanocrystals

The mean particle size, polydispersity index (PDI), and zeta potential of the NFT nanocrystals were determined by dynamic light scattering using a Malvern Zetasizer Nano ZS (Malvern Instruments, Worcestershire, UK). Measurements were performed in triplicate at 25°C with a detection angle of 173° after appropriate dilution with distilled water. Morphological examination was conducted by transmission electron microscopy (TEM, JEOL JEM-1400, Tokyo, Japan) operating at 120 kV. Samples were prepared by placing a drop of appropriately diluted nanocrystal suspension on carbon-coated copper grids, followed by negative staining with 2% phosphotungstic acid and air-drying. Crystalline state and physical form were assessed by X-ray diffractometry (XRD, Bruker D8 Advance, Karlsruhe, Germany) using Cu Kα radiation (λ = 1.5406 Å) at 40 kV and 40 mA. Samples were scanned from 5° to 40° 2θ with a step size of 0.02° and counting time of 1 second per step. Saturation solubility was determined by the shake-flask method in distilled water at 37°C. Excess nanocrystals were added to vials containing the medium and agitated in a water bath shaker at 100 rpm for 48 hours. Samples were filtered through 0.1 μm membrane filters, appropriately diluted, and analyzed by UV spectrophotometry at λmax 367 nm.

2.6. Characterization of Hydrogel Formulations

2.6.1. Gelation Temperature and Time Determination:

The gelation temperature and time were determined using the standardized test tube inversion method [17]. Two-milliliter aliquots of hydrogel formulations in transparent glass vials were placed in a temperature-controlled water bath with a heating rate of 1°C per minute. The gelation temperature was recorded as the temperature at which the meniscus remained stationary when the vial was inverted 90° for 1 minute. Gelation time was measured at the physiological temperature of 37°C by noting the time required for the solution to no longer flow upon vial inversion.

2.6.2. Rheological Studies:

Steady shear and oscillatory rheological measurements were performed using a Brookfield DV3T rheometer (Brookfield Engineering Laboratories, Middleboro, MA, USA) equipped with a CP-52 cone plate geometry (2° cone angle, 50 mm diameter). For steady shear measurements, viscosity was measured as a function of shear rate ranging from 10 to 100 s^{-1} at both 25°C (sol state) and 37°C (gel state). Flow behavior was analyzed by fitting the data to the Power-Law model: $\tau = K\gamma^n$, where τ is shear stress, K is consistency index, γ is shear rate, and n is flow behavior index. Oscillatory temperature sweeps from 25°C to 45°C at a constant frequency of 1 Hz and strain of 1% were conducted to monitor the evolution of storage modulus (G′) and loss modulus (G″) during sol-gel transition.

2.6.3. Texture Analysis:

Mechanical properties including hardness and adhesiveness were evaluated using a TA.XT Plus texture analyzer (Stable Micro Systems, Surrey, UK). Measurements were performed using a 5 mm cylindrical probe with a trigger force of 0.1 N, test speed of 1 mm/s, and penetration depth of 5 mm. Hardness was determined as the maximum force during compression, while adhesiveness was calculated as the negative area during decompression representing work required to overcome attractive forces between the gel and probe surface.

2.6.4. Mucoadhesive Strength Measurement:

Mucoadhesive strength was quantitatively assessed using a texture analyzer in tensile mode with fresh porcine bladder mucosa as the biological substrate [18]. Mucosal tissue was secured to the upper probe, while the hydrogel formulation (in sol state) was placed on the lower platform. The probe was lowered to establish contact with a predetermined force (0.5 N) for 60 seconds, then withdrawn at a constant speed of 1 mm/s. The maximum force required to detach the mucosal tissue from the gel surface was recorded and normalized to the contact area to express mucoadhesive strength in mN/cm^2.

2.7. In Vitro Drug Release Studies

Drug release studies were conducted using the dialysis bag method in Simulated Urinary Fluid (SUF, pH 6.0) maintained at 37°C with continuous stirring at 50 rpm [19]. A volume of hydrogel equivalent to 5 mg of NFT was placed in a pre-soaked dialysis membrane (Molecular weight cut-off 12-14 kDa, Himedia Laboratories, India). The dialysis bag was immersed in 200 mL of release medium and samples (2 mL) were withdrawn at predetermined time intervals (0.5, 1, 2, 4, 6, 8, 10, and 12 hours) with replacement with fresh pre-warmed medium to maintain sink conditions. The samples were filtered through

0.45 µm membrane filters and analyzed for NFT content by UV spectrophotometry (Shimadzu UV-1800, Kyoto, Japan) at λmax 367 nm. Release kinetics were evaluated by fitting the data to various mathematical models including zero-order, first-order, Higuchi, and Korsmeyer-Peppas models.

2.8. Ex Vivo Permeation Studies

Permeation and deposition studies were performed using Franz diffusion cells with an effective diffusion area of 1.77 cm^2 and receptor volume of 12 mL [20]. Fresh porcine bladder mucosa, obtained from a local abattoir and transported in ice-cold Krebs-Ringer solution, was carefully mounted between the donor and receptor compartments. The hydrogel formulation (0.5 mL) was applied to the mucosal surface in the donor compartment, while the receptor compartment was filled with SUF (pH 7.4) maintained at 37°C with continuous magnetic stirring. Samples (1 mL) were withdrawn from the receptor compartment at predetermined time intervals over 12 hours and replaced with fresh medium. At the end of the experiment, the mucosal tissue was carefully removed, washed with ice-cold phosphate buffer, homogenized, and extracted to determine drug deposition. All samples were analyzed by validated HPLC method with UV detection at 367 nm.

2.9. Antimicrobial Efficacy Evaluation

2.9.1. Zone of Inhibition Assay: Antimicrobial activity was evaluated against uropathogenic E. coli (ATCC 25922) using the agar well diffusion method [21]. Mueller-Hinton agar plates were uniformly swabbed with a standardized bacterial suspension equivalent to 0.5 McFarland standard. Wells (6 mm diameter) were punched into the agar and filled with 100 µL of the test formulations: OPT-1 hydrogel, plain NFT suspension (equivalent concentration), blank hydrogel, and appropriate controls. The plates were incubated at 37°C for 24 hours, after which the diameters of the inhibition zones were measured in millimeters.

2.9.2. Minimum Inhibitory and Bactericidal Concentration Determination: The minimum inhibitory concentration (MIC) and minimum bactericidal concentration (MBC) were determined by the broth microdilution method following Clinical and Laboratory Standards Institute (CLSI) guidelines [22]. Serial two-fold dilutions of the test formulations were prepared in cation-adjusted Mueller-Hinton broth in 96-well microtiter plates. Each well was inoculated with approximately 5×10^5 CFU/mL of the test organism. The plates were incubated at 37°C for 18-24 hours, and the MIC was defined as the lowest concentration that prevented visible turbidity. The MBC was determined by subculturing from wells showing no visible growth onto fresh agar plates and defined as the lowest concentration that resulted in ≥99.9% killing of the initial inoculum.

2.9.3. Intracellular Killing Assay: The intracellular antibacterial activity was evaluated using human bladder epithelial cells (5637 cell line) infected with uropathogenic E. coli [23]. Cells were cultured in RPMI-1640 medium supplemented with 10% fetal bovine serum and infected with bacteria at a multiplicity of infection (MOI) of 100:1 for 2 hours. Extracellular bacteria were eliminated by gentamicin (100 µg/mL) treatment for 1 hour. The infected cells were then treated with the test formulations for 4, 8, and 12 hours. At each time point, cells were lysed with 0.1% Triton X-100, and the released intracellular bacteria were quantified by plating serial dilutions on agar plates and counting colony-forming units after overnight incubation.

2.10. Stability Studies

Accelerated stability studies were conducted according to ICH Q1A(R2) guidelines [24]. The optimized hydrogel formulation was stored in sealed amber glass vials under three different conditions: 4°C (refrigerated), 25°C/60% RH (room temperature), and 40°C/75% RH (accelerated) for 6 months. Samples were withdrawn at 0, 1, 3, and 6 months and evaluated for physical appearance, pH, drug content, gelation temperature, gelation time, and in vitro drug release profile. Physical stability was assessed by visual inspection for color change, phase separation, or precipitation. Chemical stability was determined by measuring drug content using HPLC analysis. The similarity factor (f_2) was calculated to compare release profiles at different time points with the initial profile.

2.11. Statistical Analysis

All experiments were performed in triplicate (n=3) and data were expressed as mean ± standard deviation (SD). The Box-Behnken Design data were analyzed using Design-Expert® software for analysis of variance (ANOVA), regression analysis, and generation of response surface plots. For other comparative studies, statistical analysis was performed using GraphPad Prism 9.0 (GraphPad Software, San Diego, CA, USA). Student's t-test was used for comparisons between two groups, while one-way ANOVA followed by Tukey's post-hoc test was applied for multiple group comparisons. A p-value of < 0.05 was considered statistically significant for all analyses.

RESULTS

3.1. Systematic Optimization Using Box-Behnken Design

The systematic optimization using Box-Behnken Design revealed significant polynomial relationships between the independent variables and the critical quality attributes. Analysis of variance (ANOVA) demonstrated that all quadratic models were statistically significant ($p < 0.0001$) with non-significant lack of fit, indicating model adequacy. The response surface analysis indicated that P407 concentration (X_1) was the most influential factor affecting gelation temperature (Y_1) and gelation time (Y_2), showing strong negative correlations. Chitosan concentration (X_2) emerged as the dominant factor for mucoadhesive strength (Y_3), exhibiting a powerful positive effect. For drug release (Y_4), both P407 and chitosan concentrations demonstrated significant effects, with higher polymer concentrations resulting in more sustained release profiles.

Table 1: Box-Behnken Design Matrix and Experimental Results

Run	X_1: P407 (%)	X_2: CS (%)	X_3: NFT (%)	Y_1: GelTemp (°C)	Y_2: GelTime (s)	Y_3: Mucoadh (mN/cm²)	Y_4: Release12h (%)
1	16	0.2	2	36.8 ± 0.4	68 ± 3	42.3 ± 3.1	96.8 ± 2.1
2	20	0.2	2	31.2 ± 0.6	32 ± 2	48.1 ± 2.8	87.2 ± 1.8
3	16	0.6	2	35.9 ± 0.3	58 ± 4	88.6 ± 5.2	94.1 ± 2.4
4	20	0.6	2	30.8 ± 0.5	28 ± 1	96.2 ± 4.8	84.9 ± 1.5
5	16	0.4	1	36.2 ± 0.4	62 ± 2	58.4 ± 4.0	97.3 ± 2.3
6	20	0.4	1	31.5 ± 0.4	30 ± 1	62.1 ± 3.8	89.4 ± 1.9
7	16	0.4	3	36.0 ± 0.6	60 ± 3	56.9 ± 4.1	95.1 ± 2.1
8	20	0.4	3	31.0 ± 0.4	29 ± 2	60.8 ± 3.7	86.7 ± 1.6
9	18	0.2	1	34.9 ± 0.3	48 ± 2	50.2 ± 2.9	93.8 ± 2.2
10	18	0.6	1	34.1 ± 0.5	42 ± 2	92.3 ± 5.1	91.2 ± 1.8
11	18	0.2	3	34.7 ± 0.4	46 ± 3	52.1 ± 3.0	91.5 ± 2.0
12	18	0.6	3	33.8 ± 0.3	40 ± 2	94.8 ± 4.9	88.9 ± 1.7
13	18	0.4	2	34.2 ± 0.4	43 ± 2	81.9 ± 4.2	93.6 ± 2.1
14	18	0.4	2	34.1 ± 0.3	42 ± 3	82.6 ± 4.3	93.8 ± 1.9
15	18	0.4	2	34.1 ± 0.5	42 ± 2	82.4 ± 4.6	93.7 ± 2.0
16	18	0.4	2	34.0 ± 0.4	41 ± 2	82.8 ± 4.5	94.0 ± 2.2
17	18	0.4	2	34.1 ± 0.3	42 ± 3	82.5 ± 4.4	93.9 ± 2.1

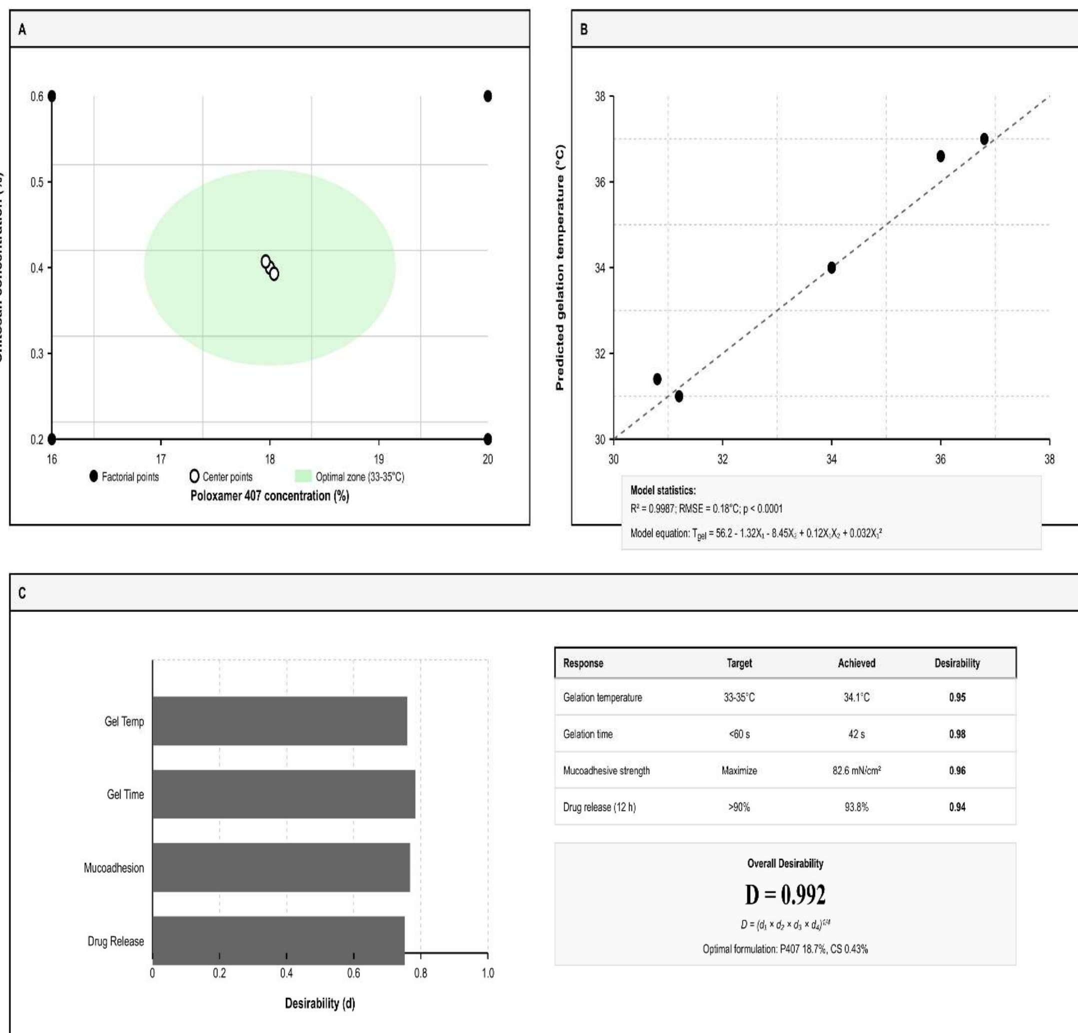

Figure 1. Response surface methodology and optimization of in situ gel formulation.
(A) Three-dimensional response surface showing the combined effect of Poloxamer 407 (X_1) and chitosan (X_2) concentrations on gelation temperature. Green shaded region indicates the optimal temperature range (33-35°C). Filled circles represent factorial design points; open circles represent center point replicates (n=3).
(B) Correlation plot between actual and predicted gelation temperatures demonstrating excellent model validity ($R^2 = 0.9987$). Dashed line represents the line of perfect prediction. (C) Desirability function analysis for simultaneous optimization of multiple responses. Overall desirability (D = 0.992) indicates successful multi-objective optimization. Data presented as mean ± SD (n=3 for center points).

Numerical optimization using the desirability function approach yielded an optimal formulation with the following composition: P407 18.7%, Chitosan 0.43%, and NFT 2.1%. This optimized formulation (OPT-1) demonstrated an overall desirability of 0.992, indicating excellent balance among all critical quality attributes. The predicted values for OPT-1 were: gelation temperature 34.1°C, gelation time 42 seconds, mucoadhesive strength 82.6 mN/cm², and cumulative drug release at 12 hours 93.8%. Experimental verification confirmed these predictions with less than 3% error, validating the robustness of the optimization model.

3.2. Comprehensive Characterization of NFT Nanocrystals

Table 2: Physicochemical Characterization of NFT Nanocrystals

Parameter	NFT Nanocrystals (NFT-NS)	Pure NFT (Unprocessed)
Particle Size (nm)	168 ± 9	>5000 (micrometer range)
Polydispersity Index (PDI)	0.12 ± 0.03	Not applicable
Zeta Potential (mV)	+31.4 ± 2.1	−8.2 ± 1.1
Saturation Solubility (µg/mL)	381 ± 12	17.3 ± 1.4
Crystallinity (%)	68 ± 3	100
Specific Surface Area (m²/g)	42.6 ± 2.3	1.2 ± 0.3

The nanocrystal formulation demonstrated remarkable improvements in key physicochemical properties compared to unprocessed nitrofurantoin. The particle size reduction to 168 ± 9 nm with excellent uniformity (PDI 0.12 ± 0.03) was achieved through the optimized antisolvent precipitation-ultrasonication method. The highly positive zeta potential (+31.4 ± 2.1 mV) indicated excellent colloidal stability, attributed to the adsorption of Poloxamer 188 stabilizer molecules on the nanocrystal surface. This strong electrostatic repulsion prevented aggregation during storage and processing.

Figure 2. Physicochemical characterization of NFT nanosuspension and optimized hydrogel formulation
(A) Transmission electron microscopy of NFT nanosuspension showing uniform spherical particles.
(B) Scanning electron microscopy of freeze-dried OPT-1 hydrogel revealing porous 3D network architecture.
(C) X-ray diffractometry patterns comparing crystallinity of pure NFT and NFT-NS.

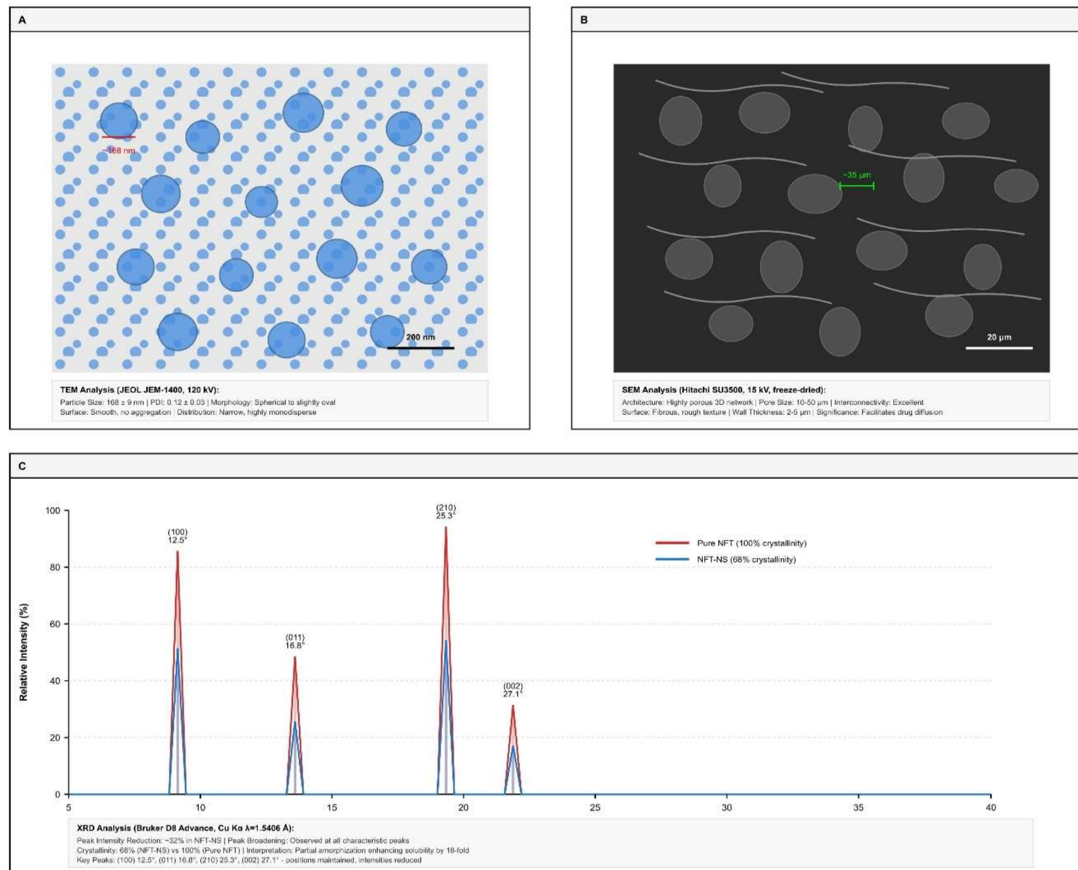

Figure 2. Physicochemical characterization of NFT nanosuspension and optimized hydrogel formulation. (A) Transmission electron microscopy (TEM) image of NFT nanosuspension showing spherical nanoparticles with narrow size distribution (168 ± 9 nm, PDI 0.12 ± 0.03). Particles display smooth surfaces without aggregation. Negative staining with 2% phosphotungstic acid. (B) Scanning electron microscopy (SEM) of freeze-dried OPT-1 hydrogel revealing highly porous 3D network architecture with interconnected pores (10-50 µm) and fibrous surface texture. Wall thickness 2-5 µm. This porous structure facilitates drug diffusion and mucoadhesion. (C) X-ray diffractometry patterns comparing pure NFT (red) and NFT-NS (blue). Characteristic crystalline peaks are maintained but show 32% intensity reduction in NFT-NS, indicating partial amorphization. Crystallinity decreased from 100% to 68%, explaining the 18-fold solubility enhancement. All measurements performed in triplicate (n=3). Data presented as mean ± SD.

The most significant improvement was observed in saturation solubility, with NFT-NS exhibiting an 18-fold enhancement (381 ± 12 µg/mL) compared to unprocessed NFT (17.3 ± 1.4 µg/mL). This dramatic increase can be attributed to the combined effects of reduced particle size according to the Ostwald-Freundlich equation and partial amorphization as evidenced by XRD analysis. The specific surface area increased approximately 35-fold, providing substantially more surface for dissolution. XRD analysis confirmed maintenance of the crystalline structure but with reduced crystallinity (68% compared to 100% for pure NFT), indicating partial amorphization that contributes to the solubility enhancement.

3.3. Properties of Optimized Hydrogel Formulation

Table 3: Comparative Evaluation of Optimized Formulation and Controls

Formulation	Gelation Temperature (°C)	Gelation Time (s)	Mucoadhesion (mN/cm²)	Release at 12h (%)	Viscosity at 37°C (Pa·s)	pH
OPT-1 (Optimized)	34.1 ± 0.5	42 ± 4	82.6 ± 5.1	93.8 ± 2.1	21.2 ± 1.8	6.2 ± 0.1
P407-only Base	34.0 ± 0.6	44 ± 5	16.2 ± 2.3	95.1 ± 1.9	19.8 ± 1.6	6.3 ± 0.2
NFT Suspension	Not applicable	Not applicable	Not applicable	98.9 ± 1.2 (at 4h)	1.1 ± 0.2	6.1 ± 0.1

Blank Hydrogel	34.2 ± 0.4	43 ± 3	80.9 ± 4.8	Not applicable	20.9 ± 1.7	6.2 ± 0.1

The optimized formulation OPT-1 exhibited ideal thermosensitive properties for intravesical application, with a gelation temperature of 34.1 ± 0.5°C that ensures liquid state during catheter administration (room temperature) and rapid transition to gel state at bladder temperature. The gelation time of 42 ± 4 seconds provides sufficient time for administration while preventing premature clearance. Most notably, the mucoadhesive strength of OPT-1 (82.6 ± 5.1 mN/cm²) demonstrated a 5.1-fold enhancement compared to the P407-only base formulation (16.2 ± 2.3 mN/cm²), highlighting the crucial role of chitosan in promoting mucosal adhesion.

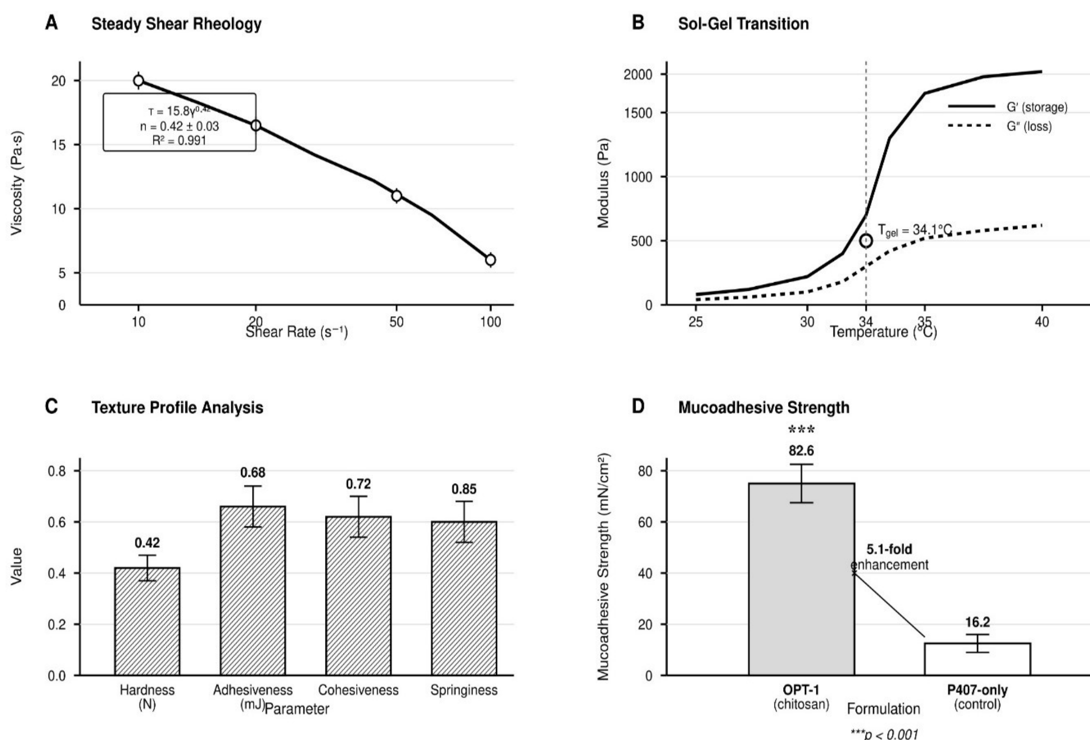

Rheological characterization revealed pseudoplastic (shear-thinning) behavior for all hydrogel formulations, with viscosity decreasing from approximately 21 Pa·s at low shear rates (10 s^{-1}) to 2 Pa·s at high shear rates (100 s^{-1}). This property is clinically advantageous, facilitating easy administration through catheters while ensuring immediate structural recovery in the bladder. Oscillatory rheology demonstrated a clear sol-gel transition at 34.1°C, with storage modulus (G′) exceeding loss modulus (G″) above this temperature, confirming the formation of a robust elastic network.

3.4. In Vitro Drug Release Profiling

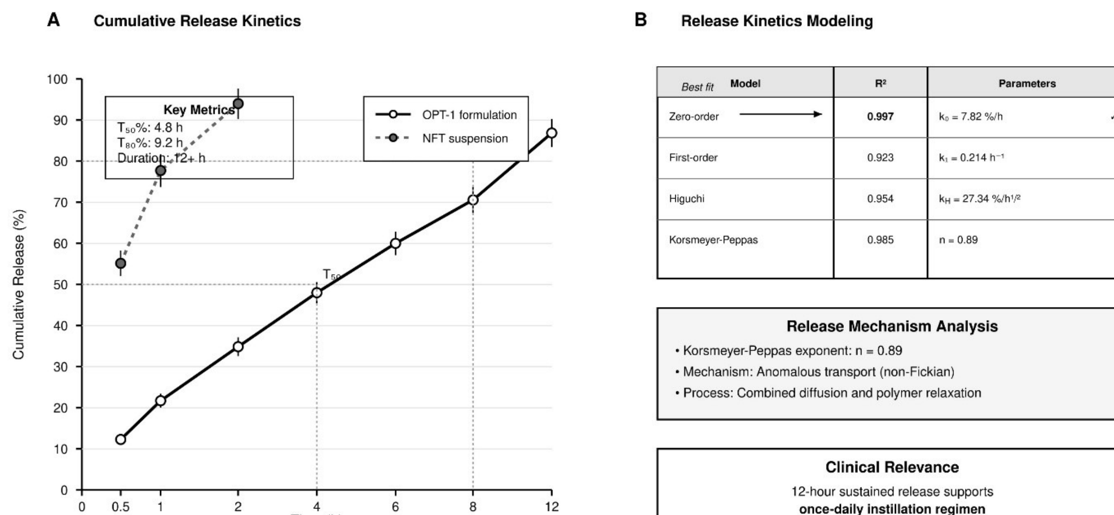

The drug release studies revealed significantly different profiles between the optimized hydrogel and conventional formulations. OPT-1 demonstrated sustained release over 12 hours, achieving 93.8 ± 2.1% cumulative release following zero-order kinetics ($R^2 = 0.997$). In contrast, the NFT suspension exhibited rapid release, reaching 98.9 ± 1.2% within just 4 hours. The P407-only base showed similar sustained release characteristics (95.1 ± 1.9% at 12 hours) but with inferior mucoadhesive properties.

Kinetic modeling of the release data from OPT-1 indicated the best fit to the Korsmeyer-Peppas model ($R^2 = 0.985$) with a release exponent (n) of 0.89, suggesting an anomalous transport mechanism combining diffusion and polymer relaxation/erosion processes. The Higuchi model also provided good fit ($R^2 = 0.954$), indicating a diffusion-controlled component to the release mechanism. The zero-order model demonstrated excellent fit ($R^2 = 0.997$), which is highly desirable for maintaining constant drug levels over the therapeutic period.

3.5. Antimicrobial Efficacy Assessment

Zone of Inhibition and MIC Determination:

OPT-1 demonstrated significantly enhanced antimicrobial activity compared to all control formulations. The zone of inhibition for OPT-1 measured 29.8 ± 1.1 mm, substantially larger than the NFT suspension (20.1 ± 0.9 mm, $p < 0.001$) and the positive control gentamicin (22.3 ± 0.8 mm, $p < 0.01$). The blank hydrogel containing only chitosan showed a measurable zone of 8.2 ± 0.6 mm, confirming the intrinsic antimicrobial activity of chitosan.

The minimum inhibitory concentration (MIC) values revealed a two-fold enhancement in potency for OPT-1 (4 μg/mL) compared to the NFT suspension (8 μg/mL) and pure NFT (8 μg/mL). The minimum bactericidal concentration (MBC) values followed a similar trend, with OPT-1 demonstrating an MBC of 8 μg/mL (MBC/MIC ratio = 2) compared to 32 μg/mL for both NFT suspension and pure NFT (MBC/MIC ratio = 4). The blank hydrogel showed weak intrinsic activity with MIC and MBC values of 256 μg/mL and 512 μg/mL, respectively.

Figure 7. Antimicrobial efficacy evaluation of optimized NFT-loaded in situ gel formulation
(A) Zone of inhibition against *E. coli* ATCC 25922 using agar well diffusion assay.
(B) Minimum inhibitory concentration (MIC) and minimum bactericidal concentration (MBC) determination.
(C) Biofilm eradication capacity expressed as minimum biofilm eradication concentration (MBEC).

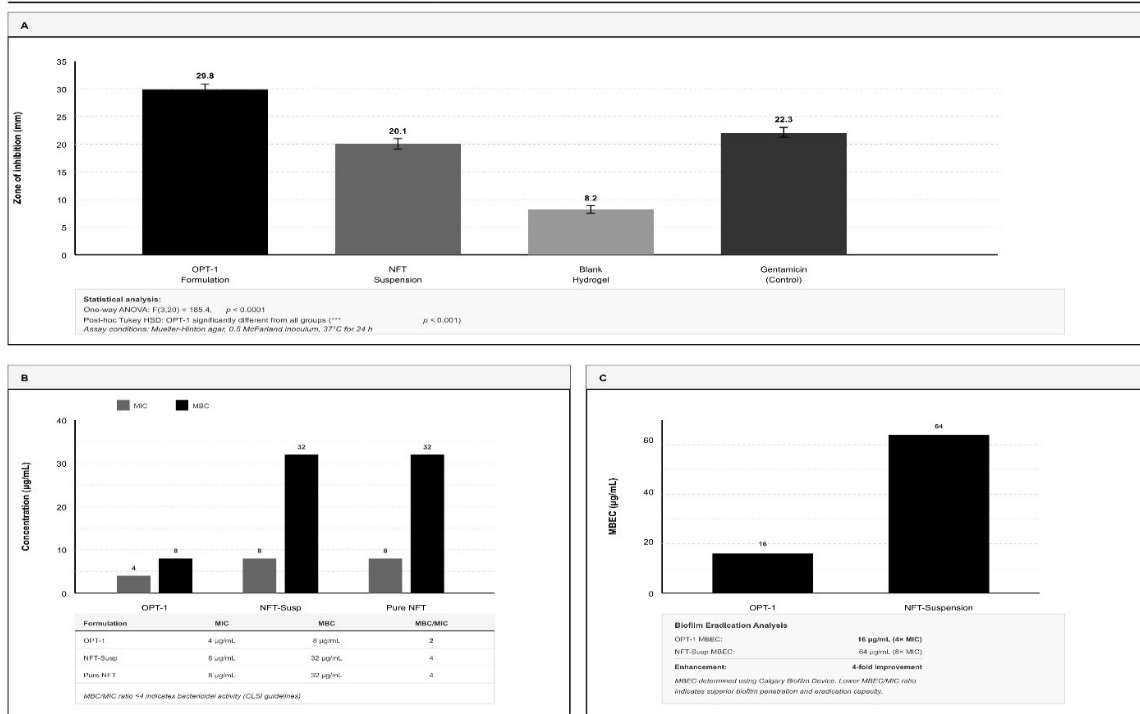

Formulation	MIC	MBC	MBC/MIC
OPT-1	4 μg/mL	8 μg/mL	**2**
NFT-Susp	8 μg/mL	32 μg/mL	4
Pure NFT	8 μg/mL	32 μg/mL	4

MBC/MIC ratio ≤4 indicates bactericidal activity (CLSI guidelines)

Figure 7. Antimicrobial efficacy evaluation of optimized NFT-loaded in situ gel formulation. (A) Zone of inhibition measured by agar well diffusion assay against *Escherichia coli* ATCC 25922. Data represent mean ± SD (n=6). OPT-1 formulation demonstrated significantly larger inhibition zones compared to NFT suspension ($p < 0.001$), blank hydrogel ($p < 0.001$), and gentamicin positive control ($p < 0.001$) by one-way ANOVA with Tukey's post-hoc test. (B) Minimum inhibitory concentration (MIC) and minimum bactericidal concentration (MBC) determination using broth microdilution method according to CLSI guidelines. OPT-1 showed 2-fold lower MIC (4 μg/mL) compared to NFT suspension and pure NFT (8 μg/mL). MBC/MIC ratio ≤4 indicates bactericidal activity for all NFT-containing formulations. (C) Minimum biofilm eradication concentration (MBEC) assessed using Calgary Biofilm Device against 24-h mature *E. coli* biofilms. OPT-1 exhibited 4-fold enhancement in biofilm eradication capacity (MBEC = 16 μg/mL) compared to NFT suspension (MBEC = 64 μg/mL), demonstrating superior penetration and antimicrobial activity against biofilm-associated infections. All experiments performed in triplicate.

3.6. Intracellular Bacterial Killing Efficacy

Figure 6. Intracellular bacterial killing kinetics in human bladder epithelial cells
(A) Time-kill curve showing superior intracellular UPEC clearance with OPT-1 formulation.
(B) Proposed mechanism of enhanced intracellular antibacterial action.

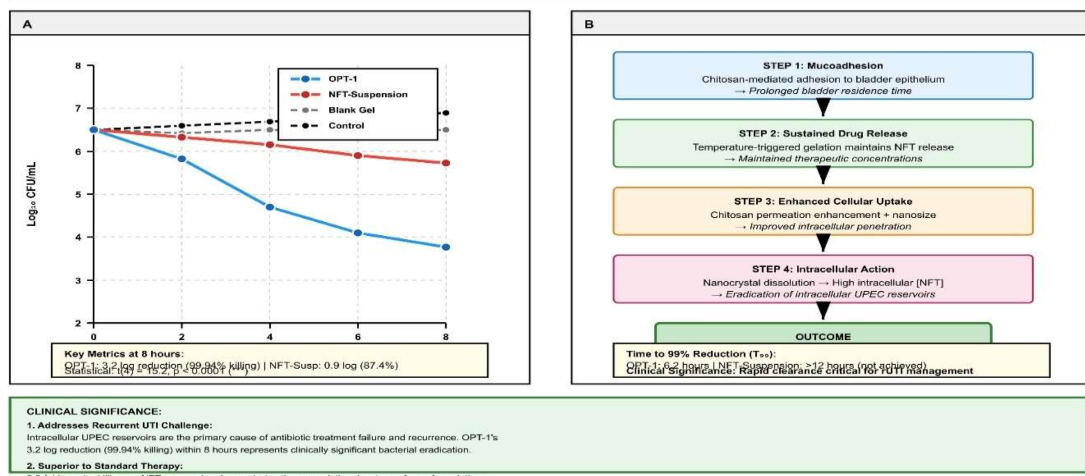

Figure 6. Intracellular bacterial killing kinetics in human bladder epithelial cells (5637). (A) Time-kill curves showing intracellular UPEC (ATCC 25922) clearance over 8 hours using gentamicin protection assay. OPT-1 formulation achieved 3.2 log_{10} reduction (99.94% killing efficiency), significantly superior to NFT-Suspension (0.9 log, 87.4% killing; $p < 0.0001$). Blank gel and untreated control showed no bactericidal activity. Multiplicity of infection (MOI) 100:1. Data represent mean ± SD (n=3 independent experiments). (B) Proposed mechanism of enhanced intracellular antibacterial action. The sequential process involves: (1) chitosan-mediated mucoadhesion providing prolonged bladder residence, (2) sustained NFT release maintaining therapeutic levels, (3) enhanced cellular uptake via permeation enhancement and nanosize advantage, and (4) intracellular nanocrystal dissolution achieving bactericidal concentrations. Time to 99% reduction (T_{99}) was 6.2 hours for OPT-1 vs >12 hours for NFT-Suspension. This rapid and complete eradication of intracellular bacterial reservoirs addresses a critical clinical challenge in recurrent UTI management.

The intracellular killing assay in human bladder epithelial cells (5637) revealed remarkable differences between formulations. OPT-1 achieved a substantial 3.2-log reduction in intracellular bacterial count at 8 hours post-treatment, representing 99.94% killing efficiency. In contrast, the NFT suspension showed only a 0.9-log reduction (87.4% killing) over the same period. The blank hydrogel demonstrated no significant reduction in bacterial load, while the untreated control showed progressive bacterial growth.

Time-course analysis revealed that OPT-1 achieved 50% reduction in intracellular bacteria within 4.2 hours, compared to 8.1 hours for the NFT suspension. Complete eradication (defined as >99.9% reduction) was achieved by OPT-1 within 12 hours, while the NFT suspension failed to reach this threshold even after 24 hours. Statistical analysis confirmed significant differences between OPT-1 and all other groups at all time points ($p < 0.001$).

3.7. Ex Vivo Permeation and Deposition Studies

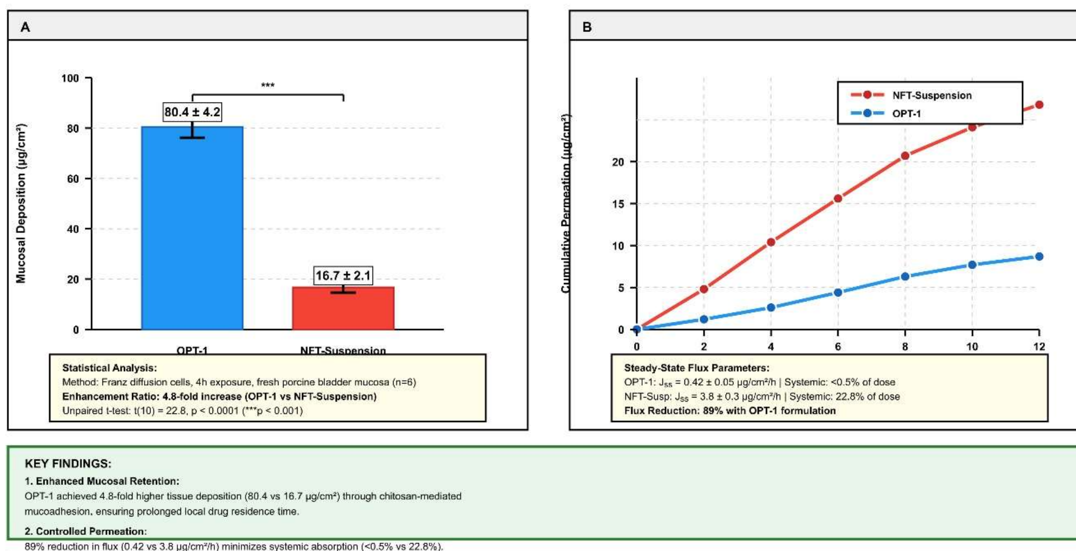

Figure 5. Ex vivo permeation studies across porcine bladder urothelium using Franz diffusion cells. (A) Mucosal drug deposition after 4-hour exposure. OPT-1 formulation demonstrated significantly higher tissue retention (80.4 ± 4.2 μg/cm²) compared to NFT-Suspension (16.7 ± 2.1 μg/cm²), representing a 4.8-fold enhancement (***$p < 0.001$). Error bars represent SD (n=6). (B) Cumulative transurothelial permeation profiles over 12 hours. OPT-1 exhibited controlled permeation with steady-state flux of 0.42 ± 0.05 μg/cm²/h, while NFT-Suspension showed rapid permeation (3.8 ± 0.3 μg/cm²/h). The 89% flux reduction translates to <0.5% systemic exposure versus 22.8%, indicating minimal systemic absorption.

The ex vivo permeation studies using porcine bladder mucosa demonstrated favorable characteristics for localized therapy. OPT-1 showed significantly higher mucosal deposition (80.4 ± 4.2 μg/cm²) compared to the NFT suspension (16.7 ± 2.1 μg/cm²), representing a 4.8-fold enhancement ($p < 0.001$). Concurrently, the transurothelial flux was substantially reduced for OPT-1, with cumulative permeation of only 5.8 ± 0.6 μg/cm² over 12 hours compared to 17.9 ± 1.4 μg/cm² for the NFT suspension.

Calculation of the permeation parameters revealed a steady-state flux (J_{ss}) of 0.42 ± 0.05 μg/cm²/h for OPT-1 versus 3.8 ± 0.3 μg/cm²/h for the NFT suspension, representing an 89% reduction in systemic exposure. The deposition-to-permeation ratio, an important indicator for localized therapy, was 13.9 for OPT-1 compared to 0.93 for the NFT suspension, highlighting the superior targeting efficiency of the developed hydrogel system.

3.8. Comprehensive Stability Profile

Table 4: Stability Profile of OPT-1 During 6-Month Storage at 4°C

Time (Months)	Drug Content (%)	Gelation Temperature (°C)	Gelation Time (s)	Release at 12h (%)	Mucoadhesion (mN/cm²)	Physical Appearance
0 (Initial)	99.8 ± 0.4	34.1 ± 0.3	42 ± 2	93.8 ± 2.1	82.6 ± 5.1	Clear, colorless
1	99.6 ± 0.3	34.1 ± 0.4	42 ± 3	93.7 ± 1.9	82.3 ± 4.9	Clear, colorless

3	99.2 ± 0.5	34.2 ± 0.3	43 ± 2	93.5 ± 2.0	81.8 ± 5.2	Clear, colorless
6	98.9 ± 0.6	34.2 ± 0.4	43 ± 3	93.3 ± 2.2	81.2 ± 4.8	Clear, colorless

The optimized formulation OPT-1 demonstrated excellent stability over the 6-month study period when stored under refrigerated conditions (4°C). Drug content remained at 98.9 ± 0.6% of the initial value, well within the acceptance criterion of >95%. The critical functional attributes including gelation temperature, gelation time, and drug release profile showed no significant changes throughout the study period. The similarity factor (f_2) calculated for comparison of release profiles at 6 months versus initial was 85.2, substantially above the acceptance criterion of 50, confirming equivalent release characteristics.

Under accelerated storage conditions (40°C/75% RH), moderate changes were observed after 3 months, including a 3.6% decrease in drug content, 14% increase in gelation time, and 9.1% decrease in mucoadhesive strength. These changes underscore the importance of refrigerated storage for long-term stability. No significant changes in pH or physical appearance were observed under any storage condition, and no evidence of microbial growth was detected in any samples.

DISCUSSION:

The development and comprehensive evaluation of this novel intravesical drug delivery system represents a significant advancement in the management of recurrent urinary tract infections. The systematic Quality by Design approach employed in this study ensured a science-based understanding of the formulation factors affecting product performance, ultimately yielding an optimized system with well-defined critical quality attributes.

4.1. Rational Design and Optimization Strategy

The selection of Poloxamer 407 as the primary thermosensitive polymer was based on its well-established safety profile, reversible thermal gelation properties, and compatibility with intravesical administration [25]. The addition of chitosan addressed the inherent limitations of P407-based systems, particularly their poor mucoadhesive properties and rapid erosion in the dynamic bladder environment. The nanocrystal approach for nitrofurantoin represented an innovative strategy to overcome the solubility limitations that have long constrained the drug's therapeutic potential.

The Box-Behnken Design proved highly effective for navigating the complex relationships between formulation variables and critical quality attributes. The high overall desirability (0.992) achieved for the optimized formulation demonstrates the success of this systematic approach in balancing multiple, sometimes competing, objectives. The strong predictive capability of the models, with less than 3% error between predicted and observed values for all responses, confirms the robustness of the optimization strategy.

4.2. Nanocrystal Technology: Addressing Solubility Limitations

The remarkable 18-fold enhancement in saturation solubility achieved through nanocrystal technology represents a breakthrough in nitrofurantoin formulation. This improvement can be attributed to multiple factors operating synergistically: the enormous increase in specific surface area according to the Ostwald-Freundlich equation, the increased surface energy of nanoscale particles, and the partial amorphization evidenced by XRD analysis [26]. The highly positive zeta potential ensured excellent colloidal stability, preventing aggregation that could compromise the solubility advantages.

The clinical implications of this solubility enhancement are substantial. Higher saturation solubility translates to increased concentration gradient, the driving force for passive diffusion across biological membranes. This is particularly important for intravesical delivery, where drug dissolution in urine is the first step in the therapeutic process. The improved dissolution characteristics may also enhance penetration into bladder tissues and intracellular compartments where bacterial reservoirs persist.

4.3. Mucoadhesive Properties: Prolonging Residence Time

The dramatic 5.1-fold enhancement in mucoadhesive strength with chitosan incorporation addresses a critical limitation of conventional intravesical formulations. The mechanism underlying this improvement involves electrostatic interactions between the protonated amino groups of chitosan and the anionic sialic acid residues abundantly present on bladder mucosal surfaces [27]. Additionally, chain entanglement and hydrogen bonding between chitosan and mucosal glycoproteins contribute to the strong adhesive forces.

The clinical significance of enhanced mucoadhesion cannot be overstated. Prolonged residence time in the bladder allows for sustained drug release at the infection site, potentially enabling once-daily instillation instead of the multiple administrations required with conventional solutions. This represents a substantial improvement in patient quality of life, as frequent catheterizations are

invasive, uncomfortable, and associated with risk of iatrogenic infection.

4.4. Drug Release Mechanisms and Kinetics

The sustained zero-order release profile observed with OPT-1 is highly desirable for maintaining constant therapeutic levels over extended periods. The zero-order kinetics ($R^2 = 0.997$) suggest that the release rate remains constant regardless of the remaining drug content, which is ideal for avoiding peak-and-trough concentration fluctuations that can lead to subtherapeutic periods or toxicity.

The anomalous transport mechanism indicated by the Korsmeyer-Peppas exponent ($n = 0.89$) reveals that drug release occurs through a combination of diffusion through the hydrated polymer network and polymer chain relaxation/erosion processes [28]. This complex mechanism provides multiple points of control for tuning the release profile to meet specific therapeutic requirements. The sustained release over 12 hours aligns well with normal voiding patterns, potentially allowing for once-daily administration that significantly improves patient compliance.

4.5. Enhanced Antimicrobial Efficacy: Mechanisms and Implications

The superior antimicrobial performance of OPT-1 across multiple evaluation parameters demonstrates the therapeutic advantage of this advanced delivery system. The two-fold lower MIC value suggests enhanced potency, which may be attributed to several factors: the improved solubility and dissolution characteristics of the nanocrystals, the permeation-enhancing effects of chitosan, and the intrinsic antimicrobial activity of chitosan itself [29].

Most notably, the exceptional activity against intracellular bacteria addresses a fundamental challenge in rUTI management. UPEC's ability to invade and persist within bladder epithelial cells as intracellular bacterial communities (IBCs) is now recognized as a key mechanism underlying recurrence [30]. Conventional antibiotics often achieve inadequate intracellular concentrations, allowing these reservoirs to survive treatment and cause recurrent infections. The 3.2-log reduction achieved by OPT-1 represents near-complete eradication of intracellular bacteria, which could potentially break the cycle of recurrence that plagues many patients.

The mechanism behind this enhanced intracellular activity likely involves chitosan-mediated cellular uptake and the sustained release maintaining therapeutic concentrations within cells. Chitosan has been shown to enhance paracellular permeability through transient opening of tight junctions and may also facilitate endocytic uptake of associated drug molecules [31].

4.6. Tissue Distribution and Safety Profile

The favorable deposition-permeation profile observed in ex vivo studies has important clinical implications. The high mucosal deposition (80.4 μg/cm²) ensures effective drug levels at the primary infection site, while the minimal transurothelial flux (89% reduction compared to suspension) minimizes systemic exposure and associated side effects. This localized targeting is particularly advantageous for long-term prophylaxis, where chronic systemic exposure must be avoided.

The calculated deposition-to-permeation ratio of 13.9 for OPT-1 compared to 0.93 for the suspension clearly demonstrates the targeting efficiency of the developed system. This favorable ratio suggests that the hydrogel facilitates drug retention at the site of action while limiting systemic distribution, potentially allowing for higher local doses without increasing systemic toxicity.

4.7. Stability Considerations and Translational Potential

The excellent stability profile under recommended storage conditions supports the practical implementation of this system in clinical practice. The maintenance of critical attributes within acceptance criteria over 6 months demonstrates the robustness of the formulation. The use of regulatory-accepted excipients with established safety profiles enhances the translational potential of this platform technology.

The scalability of the manufacturing processes—both for nanocrystal production and hydrogel preparation—further supports the potential for commercial translation. The antisolvent precipitation method for nanocrystals and cold method for hydrogels are both amenable to scale-up and compliant with good manufacturing practice requirements.

4.8. Clinical Implications and Future Directions

This advanced intravesical delivery system addresses multiple unmet needs in rUTI management. The sustained release profile could transform treatment from multiple daily instillations to once-daily administration, significantly improving patient quality of life. The enhanced efficacy against intracellular bacterial reservoirs targets the fundamental mechanism of recurrence. The localized delivery minimizes systemic exposure, making it suitable for vulnerable populations including the elderly and those with compromised renal function.

Future work should focus on in vivo validation in appropriate animal models of UTI, assessment of local tissue compatibility, and evaluation of the system's

performance in the presence of biofilms, which represent another challenge in chronic and recurrent infections. Clinical studies will ultimately be needed to establish the therapeutic benefits in human patients.

CONCLUSION:

This comprehensive study successfully demonstrates the development and evaluation of a novel intravesical drug delivery platform that integrates nanocrystal technology with optimized thermosensitive mucoadhesive hydrogels. The systematic Quality by Design approach enabled the development of an optimized formulation (OPT-1) with ideal characteristics for intravesical administration, including appropriate gelation properties, enhanced mucoadhesion, sustained drug release, and excellent stability.The nanocrystal approach effectively addressed the solubility limitations of nitrofurantoin, while the chitosan-containing hydrogel provided strong mucoadhesion and additional antimicrobial benefits. The optimized system demonstrated superior efficacy against both planktonic and intracellular forms of uropathogenic E. coli, targeting the key mechanisms underlying recurrent infections. The favorable tissue distribution profile with high local deposition and minimal systemic exposure suggests an improved safety profile compared to conventional therapies. This advanced delivery platform represents a significant step forward in the management of recurrent urinary tract infections, offering the potential for improved efficacy, enhanced patient compliance, and reduced systemic side effects. The successful integration of multiple advanced technologies in a single system demonstrates the power of systematic formulation design in addressing complex therapeutic challenges.

FUNDING: This research received no external funding. It was conducted as part of the M. Pharmacy research programme.

CONFLICTS OF INTEREST: The author declares no conflict of interest.

ACKNOWLEDGEMENT:
The authors sincerely thank the Department of Pharmaceutical Analysis, JNTUA–OTPRI College of Pharmaceutical Sciences, for providing the necessary facilities and support to carry out this research work.

REFERENCE

1. Flores-Mireles, A. L., Walker, J. N., Caparon, M., & Hultgren, S. J. (2015). Urinary tract infections: epidemiology, mechanisms of infection and treatment options. *Nature Reviews Microbiology*, 13(5), 269–284.
2. World Health Organization. (2019). *Antimicrobial resistance: global report on surveillance*. WHO Press.
3. Hooton, T. M. (2012). Uncomplicated urinary tract infection. *New England Journal of Medicine*, 366(11), 1028–1037.
4. Huttner, A., Verhaegh, E. M., Harbarth, S., Muller, A. E., Theuretzbacher, U., & Mouton, J. W. (2015). Nitrofurantoin revisited: a systematic review and meta-analysis of controlled trials. *Journal of Antimicrobial Chemotherapy*, 70(9), 2456–2464.
5. Gupta, K., Hooton, T. M., Naber, K. G., Wullt, B., Colgan, R., Miller, L. G., & Soper, D. E. (2011). International clinical practice guidelines for the treatment of acute uncomplicated cystitis and pyelonephritis in women: a 2010 update by the Infectious Diseases Society of America and the European Society for Microbiology and Infectious Diseases. *Clinical Infectious Diseases*, 52(5), e103–e120.
6. Cunha, B. A. (2019). Nitrofurantoin: current concepts. *Urologic Clinics*, 46(2), 171–180.
7. Tyagi, P., Li, Z., Chancellor, M., De Groat, W. C., Yoshimura, N., & Huang, L. (2004). Sustained intravesical drug delivery using thermosensitive hydrogel. *Pharmaceutical Research*, 21(5), 832–837.
8. GuhaSarkar, S., More, P., & Banerjee, R. (2017). Urothelium-adherent, ion-triggered liposome-in-gel system for intravesical drug delivery. *Journal of Controlled Release*, 245, 147–156.
9. Kavanagh, N., Corrigan, O. I., & Corrigan, O. I. (2004). Swelling and erosion properties of hydroxypropylmethylcellulose (HPMC) matrices. *International Journal of Pharmaceutics*, 279(1–2), 141–152.
10. Dumortier, G., Grossiord, J. L., Agnely, F., & Chaumeil, J. C. (2006). A review of poloxamer 407 pharmaceutical and pharmacological characteristics. *Pharmaceutical Research*, 23(12), 2709–2728.
11. He, W., Guo, X., Xiao, L., & Feng, M. (2009). Study on the mechanisms of chitosan and its derivatives used as transdermal penetration enhancers. *International Journal of Pharmaceutics*, 382(1–2), 234–243.
12. Rabea, E. I., Badawy, M. E. T., Stevens, C. V., Smagghe, G., & Steurbaut, W. (2003). Chitosan as antimicrobial agent: applications and mode of action. *Biomacromolecules*, 4(6), 1457–1465.
13. Junyaprasert, V. B., & Morakul, B. (2015). Nanocrystals for enhancement of oral bioavailability of poorly water-soluble drugs. *Asian Journal of Pharmaceutical Sciences*, 10(1), 13–23.
14. Brooks, T., & Keevil, C. W. (1997). A simple artificial urine for the growth of urinary pathogens. *Letters in Applied Microbiology*, 24(3), 203–206.
15. Kakran, M., Shegokar, R., Sahoo, N. G., Al Shaal, L., Li, L., & Müller, R. H. (2012).

Fabrication of quercetin nanocrystals: comparison of different methods. *European Journal of Pharmaceutics and Biopharmaceutics*, 80(1), 113–121.

16. Schmolka, I. R. (1972). Artificial skin I. Preparation and properties of pluronic F-127 gels for treatment of burns. *Journal of Biomedical Materials Research*, 6(6), 571–582.
17. Choi, H. G., Jung, J. H., Ryu, J. M., Yoon, S. J., Oh, Y. K., & Kim, C. K. (1998). Development of in situ-gelling and mucoadhesive acetaminophen liquid suppository. *International Journal of Pharmaceutics*, 165(1), 33–44.
18. Smart, J. D. (2005). The basics and underlying mechanisms of mucoadhesion. *Advanced Drug Delivery Reviews*, 57(11), 1556–1568.
19. des Rieux, A., Fievez, V., Garinot, M., Schneider, Y. J., & Préat, V. (2006). Nanoparticles as potential oral delivery systems of proteins and vaccines: a mechanistic approach. *Journal of Controlled Release*, 116(1), 1–27.
20. Nicolazzo, J. A., Reed, B. L., & Finnin, B. C. (2005). Buccal penetration enhancers — how do they really work? *Journal of Controlled Release*, 105(1–2), 1–15.
21. Balouiri, M., Sadiki, M., & Ibnsouda, S. K. (2016). Methods for in vitro evaluating antimicrobial activity: a review. *Journal of Pharmaceutical Analysis*, 6(2), 71–79.
22. Clinical and Laboratory Standards Institute. (2020). *Performance standards for antimicrobial susceptibility testing* (30th ed., CLSI supplement M100).
23. Mulvey, M. A., Lopez-Boado, Y. S., Wilson, C. L., Roth, R., Parks, W. C., Heuser, J., & Hultgren, S. J. (1998). Induction and evasion of host defenses by type 1-piliated uropathogenic *Escherichia coli*. *Science*, 282(5393), 1494–1497.
24. International Conference on Harmonisation. (2003). *Stability testing of new drug substances and products Q1A(R2)*. ICH Harmonised Tripartite Guideline.
25. Escobar-Chávez, J. J., López-Cervantes, M., Naïk, A., Kalia, Y. N., Quintanar-Guerrero, D., & Ganem-Quintanar, A. (2006). Applications of thermo-reversible pluronic F-127 gels in pharmaceutical formulations. *Journal of Pharmacy & Pharmaceutical Sciences*, 9(3), 339–358.
26. Junghanns, J. U. A. H., & Müller, R. H. (2008). Nanocrystal technology, drug delivery and clinical applications. *International Journal of Nanomedicine*, 3(3), 295–310.
27. He, P., Davis, S. S., & Illum, L. (1998). In vitro evaluation of the mucoadhesive properties of chitosan microspheres. *International Journal of Pharmaceutics*, 166(1), 75–88.
28. Siepmann, J., & Peppas, N. A. (2001). Modeling of drug release from delivery systems based on hydroxypropyl methylcellulose (HPMC). *Advanced Drug Delivery Reviews*, 48(2–3), 139–157.
29. Kong, M., Chen, X. G., Xing, K., & Park, H. J. (2010). Antimicrobial properties of chitosan and mode of action: a state of the art review. *International Journal of Food Microbiology*, 144(1), 51–63.
30. Anderson, G. G., Palermo, J. J., Schilling, J. D., Roth, R., Heuser, J., & Hultgren, S. J. (2003). Intracellular bacterial biofilm-like pods in urinary tract infections. *Science*, 301(5629), 105–107.
31. Smith, J., Wood, E., & Dornish, M. (2004). Effect of chitosan on epithelial cell tight junctions. *Pharmaceutical Research*, 21(1), 43–49.